Timing of Early Developmental Events in Embryos of a Tropical Sea Urchin Echinometra mathaei

Authors: Kominami, Tetsuya, and Takata, Hiromi

Source: Zoological Science, 20(5) : 617-626

Published By: Zoological Society of Japan

URL: https://doi.org/10.2108/zsj.20.617

ZOOLOGICAL SCIENCE **20**: 617–626 (2003)

Timing of Early Developmental Events in Embryos of a Tropical Sea Urchin *Echinometra mathaei*

Tetsuya Kominami* and Hiromi Takata

Department of Biology and Earth Sciences, Faculty of Science, Ehime University, 2-5 Bunkyo-Cho, Matsuyama, 790-8577, Japan

ABSTRACT—Egg volume of a tropical sea urchin *Echinometra mathaei* is about one half that of other well-known species. We asked whether such a small size of eggs affected the timings of early developmental events or not. Cleavages became asynchronous from the 7th cleavage onward, and embryos hatched out before completion of the 9th cleavage. These timings were one cell cycle earlier than those in well-known sea urchins, raising the possibility that much earlier events, such as the increase in adhesiveness of blastomeres or the specification of dorso-ventral axis (DV-axis), would also occur earlier by one cell cycle. By examining the pseudopodia formation in dissociated blastomeres, it was elucidated that blastomeres in meso- and macromere lineages became adhesive after the 4th and 5th cleavages, respectively. From cell trace experiments, it was found that the first or second cleavage plane was preferentially employed as the median plane of embryo; the DV-axis was specified mainly at the 16-cell stage. Timings of these events were also one cell cycle earlier than those in *Hemicentrotus pulcherrimus*. The obtained results suggest that most of the early developmental events in sea urchin embryos do not depend on cleavage cycles, but on other factors, such as the nucleo-cytoplasmic ratio.

Key words: cleavage cycle, dorsoventral-axis, nucleo-cytoplasmic ratio, sea urchin, timing mechanism

INTRODUCTION

Early developmental events, such as cleavages or gastrulation, occur on a definite time schedule, provided that embryos are reared at a constant temperature. To explain such regularity in the timing of early events, existence of 'developmental timers' has been sometimes argued (Dan and Ikeda, 1971; Soll, 1979, 1983; Satoh and Ikegami, 1981b; Newport and Kirschner, 1982a; Satoh, 1985). Three factors involved in the proposed mechanisms seem to be important and to operate in a variety of developing systems. The first is the internal cytoplasmic oscillator, which is thought to begin to operate soon after fertilization. Timing of early cleavages is thought to be under the control of such a cytoplasmic oscillator (Dan and Ikeda, 1971). The second is the number of cleavage cycles or DNA replications. As shown in ascidian embryos, the process necessary for muscle cell differentiation is triggered after the occurrence of the 8th cleavage (Satoh and Ikegami, 1981a). The third is the 'nucleo-cytoplasmic ratio'. The ratio doubles at each cleavage because the volume of blastomeres is reduced to one half, while the amount of nuclear material remains constant. In *Xenopus* embryos, for example, divisions of blastomeres become abruptly asynchronous (mid-blastula transition, MBT) after 12 cycles of synchronous cleavages. The timing of MBT is directed with such nucleo-cytoplasmic ratio (Newport and Kirschner, 1982a). Concomitantly with this transition, *de novo* synthesis of RNAs starts using the zygote genome, while maternal messages are predominantly used to promote development before MBT (Newport and Kirschner, 1982b).

However, the precise mechanism of 'developmental timers' remains unclear. This is mainly due to the small quantity of available data concerning the problem. It is still necessary to know which factor is crucial in individual events in a variety of developing systems. The sea urchin embryo is a preferable material for further analysis of the timing mechanism, since many stage-specific events have been known. For example, micromeres are formed at the 4th cleavage and divide unequally at the 5th cleavage. In *Hemicentrotus pulcherrimus*, dorso-ventral axis (DV-axis) is specified at some point from the 5th to 6th cleavage (Kominami, 1988). Ciliogenesis starts after the 8th cleavage (Masuda and Sato, 1984). *Mespilia globulus* embryos, as well as other well-known sea urchin species, hatch out from the fertilization envelope after completion of the 10th cleavage (Endo, 1966). Thus, the timing of many developmental

* Corresponding author: Tel. +81-89-927-9632;
FAX. +81-89-927-9630.
E-mail: tkom@sci.ehime-u.ac.jp

events can be described in relation to the cleavage cycle.

Then, which factor is crucial in directing the timing of each event in sea urchin embryos? One of the ways to address this question is to reduce the volume of unfertilized or fertilized eggs. Interestingly, the timing of MBT in *Xenopus* embryos can be altered; if the egg cytoplasm is reduced to one half or one quarter of the initial volume, MBT is accelerated by one or two cell cycles, respectively (Newport and Kirschner, 1982a). This fact strongly suggests that the timing of MBT does not depend on the cleavage cycles, but on the 'nucleo-cytoplasmic ratio'. Unfortunately, sea urchin eggs are too small to be manipulated as done in *Xenopus* or in ascidians (Yamada and Nishida, 1999). This is one of the reasons why few studies concerning timing mechanism have been reported in sea urchin embryos, in spite of its significance. To overcome this problem, we tried to examine the early development of a tropical sea urchin *Echinometra mathaei* whose eggs are fairly small (75–80 μm in diameter); the egg volume is about one half that of *H. pulcherrimus* (about 95 μm in diameter). The eggs of *E. mathaei*, we supposed might behave just like as the *H. pulcherrimus* eggs whose cytoplasm is reduced to one half.

MATERIALS AND METHODS

Materials

Adults of the sea urchin *Echinometra mathaei* were collected at the south district of Ehime prefecture during the breeding season. Animals were kept in aquaria with circulating seawater at 20°C. Milli-pore (pore size, 0.45 μm) filtered seawater (MFSW) was supplemented with 100 units/ml Penicillin G (Meiji Seika, Tokyo) and 50 μg/ml Streptomycin sulfate (Meiji Seika). Gametes were obtained by intracoelomic injection of 0.5 M KCl. Shed oocytes were rinsed twice with MFSW and inseminated with a dilute suspension of sperm. Embryos were reared in MFSW at 24°C.

Deprivation of fertilization envelope and dissociation of embryos

Unfertilized eggs were inseminated in MFSW containing 1 mM aminotriazole (Wako Pure Chemicals, Osaka) after the method reported by Showman and Foerder (1979). About 10 min after insemination, fertilized eggs were passed through nylon mesh (pore size, 62 μm) to deprive the fertilization envelope. At appropriate stages, embryos were collected with a hand-centrifuge, and transferred into 1 M glycine (isotonic to seawater). After 10 min, embryos were dissociated into single blastomeres in a small amount of the fresh medium with several strokes of gentle pipetting. Dissociated blastomeres were mounted on a glass slide, and photographed to measure the diameters of them.

DAPI-staining

Embryos were collected in a conical tube with a hand-centrifuge and fixed with Carnoi's fixative. Before staining, embryos were rinsed twice with phosphate-buffered saline (PBS). DAPI (Sigma, MO) was dissolved in DMSO at 10 mg/ml as stock and diluted with PBS at 2 μg/ml before use. Embryos were incubated in the staining solution at room temperature for 30 min, and rinsed three times with PBS for 10 min each. The specimens were mounted on a glass slide using glycerol for clarification, and examined under an epifluorescence microscope (BX50-FLA, Olympus, Tokyo).

Count of cell number in whole embryos

Numbers of cells in whole embryos were obtained after the method of Takahashi and Okazaki (1979). Briefly, 1 g orcein (Merck, Germany) was added to 50 ml acetic acid and boiled for 30 min. After cooling, 50 ml distilled-water was added, and the solution was filtered to remove the unsolved dye. Collected embryos were fixed with Carnoi's fixative, and stained with the solution for several days. The stained embryos were mounted on a glass slide with a small drop of lactic acid (Wako Pure Chemicals), covered with a cover slip and squashed. Spread nuclei were photographed and counted on photographic prints.

Observation of primary mesenchyme cells

Embryos were collected in a conical tube with a hand-centrifuge and fixed sequentially with cold methanol and ethanol (–20°C) for 20 min each. After being rinsed twice with PBS, embryos were stained with IG9, a monoclonal antibody that specifically binds to the surface of PMCs (Kominami and Takaichi, 1998), at room temperature for 1 hr. After the primary reaction, the embryos were rinsed three times with PBS for 10 min each, and then reacted with FITC-conjugated goat anti-mouse IgG (Fab fragment) antibody (Sigma) at room temperature for 1 hr. After three times rinse with PBS, the specimens were mounted on a glass slide with a drop of glycerol and examined under an epifluorescence microscope.

Observation of pseudopodia formation

To observe the lobopodium-like pseudopodia in dissociated blastomeres, embryos deprived of fertilization envelope were incubated in Ca^{2+}, Mg^{2+}-free artificial seawater for 10 min. Then, embryos were transferred into MFSW, and incubated for 1 min (Masui and Kominami, 2001). After these treatments, embryos were dissociated into single blastomeres with several strokes of gentle pipetting. Dissociated blastomeres were transferred into a plastic dish (55 mm in diameter, non-coated, Becton Dickinson Labware, NJ), and examined every cleavage stage (from the 2nd to 6th cleavage).

Injection of Lucifer Yellow CH

Embryos deprived of fertilization envelope were allowed to develop up to the 2-cell stage. Lucifer Yellow CH (Sigma) was iontophoretically injected into one of blastomeres as described (Kominami, 1988). The dye-injected embryos were reared in the dark up to the late gastrula or early prism stage (24–28 hr postfertilization). A small drop of 10% formalin was added into the culture dish to stop the ciliary movement of the embryos. The embryos were recovered from the culture dish, and examined under an epifluorescence microscope.

RESULTS

Early development of Echinometra mathaei *embryo*

Fig. 1 illustrates the early development of *E. mathaei* embryos. Comparing the egg of well-known sea urchin species (around 100 μm in diameter), the *E. mathaei* egg is rather small (Fig. 1A). The averaged diameters and standard deviations of eggs in three batches were 75.1±1.6 (n=30), 76.2±1.3 (n=30) and 78.0±2.1 (n=30). Fertilization envelope was not highly elevated. Due to the narrow perivitelline space, blastomeres could not resume the spherical shape after cleavages (Fig. 1B). At the 4th cleavage, micromeres were formed at the vegetal pole (Fig. 1C, arrow). From the 5th cleavage onward, a narrow blastocoel was noticed. Embryos began rotation at about 8 hr, and hatched out from the fertilization envelope around 9 hr postfertilization (Fig. 1D). At 16–17 hr, ingressed PMCs became

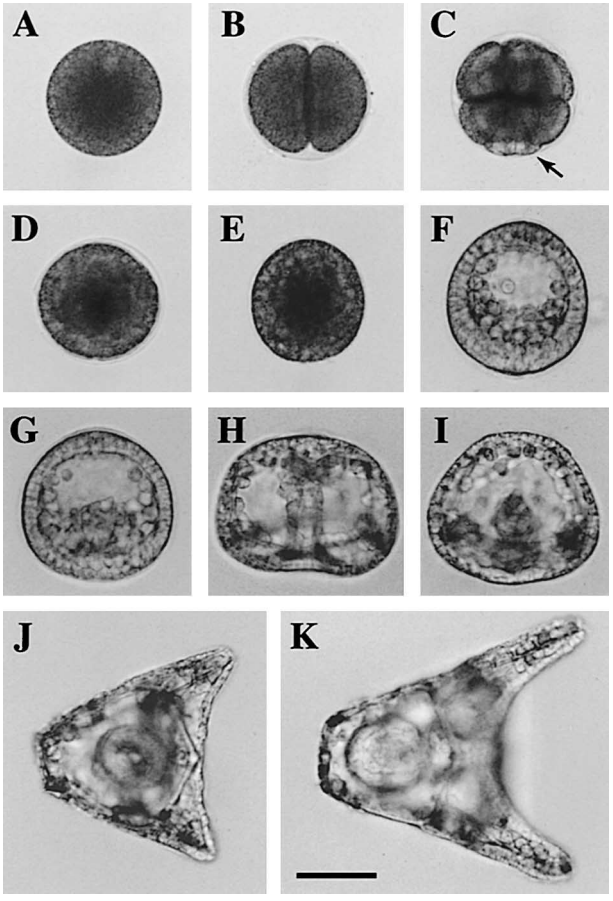

Fig. 1. *Early development of* Echinometra mathaei *embryo*
A: an unfertilized egg. B: 2-cell stage. C: 16-cell stage. D: hatching stage (9 hr postfertilization). E: a swimming blastula (12 hr), side view. F: a mesenchyme blastula (16 hr), side view. G: an early gastrula (18 hr), side view. H and I: a late gastrula (24 hr), frontal (H) and top (I) view. J: an early pluteus at 36 hr, anal view. K: a pluteus at 48 hr, anal view. An arrow in C indicates micromeres. Scale bar indicates 50 μm.

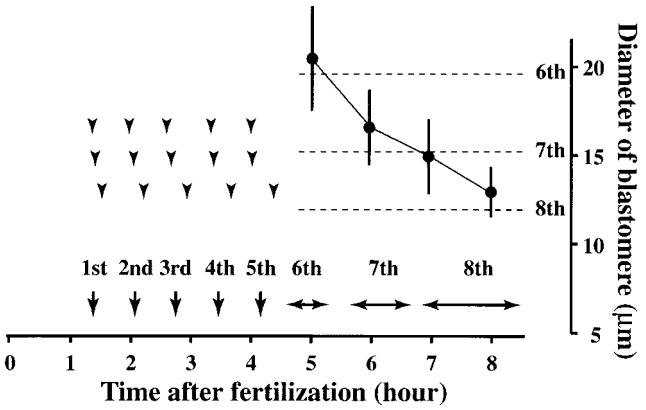

Fig. 2. *Time schedule of cleavages*
X-axis: time after fertilization (hr). Left half: timing of early cleavages. Arrowheads: timings of early (from the 1st to 5th) cleavages obtained from three batches of embryos. The averaged timing of each cleavage is indicated with an arrow accompanying the number of cleavage cycle. Right half: timing of later (from the 6th to 8th) cleavages. Y-axis: diameter of blastomeres (μm). Change in the diameter of blastomeres (solid circle) from 5 to 8 hr is shown with the standard deviation (vertical bar). Horizontal dotted lines indicate the calculated diameter of blastomeres after the completion of each cleavage. The calculation was done based on following assumptions. All blastomeres divide at each cleavage. Number of mesomere descendants is twice that of macromeres. The existence of micromere descendants is negligible, due to small number of them. The estimated duration of each cleavage is indicated with a both-sided arrow.

noticeable owing to expansion of the blastocoel (Fig. 1F). At about 18 hr, embryos started gastrulation (Fig. 1G). At 24 hr, the archenteron tip reached the apical plate (Fig. 1H). By this stage, larval skeletons had already formed, and dorsoventral axis of the embryo was clearly seen (Fig 1I). At 36 and 48 hr postfertilization, embryos developed into the early and four-armed plutei, respectively (Fig. 1J, K).

Time schedule of cleavages

Fig. 2 shows the time schedule of cleavages. Until the 5th cleavage, timing of each cleavage could be determined in intact embryos. The 1st cleavage occurred at 70–80 min postfertilization, then the 2nd to 5th cleavages followed with intervals of 40–45 min (Fig. 2, arrowheads). It is of note that formation of small micromeres was considerably delayed. Thus, the embryos were composed of 28 cells around the 4th hr of development. From the 6th cleavage onward, the timing of cleavage could not be determined in intact embryos, due to the tight adhesion of blastomeres and opaqueness of embryos. Therefore, the durations of later cleavages (Fig. 2, both-sided arrows) were estimated from the diameters of dissociated blastomeres as described below.

First, the diameters of ancestor blastomeres of each lineage, i.e., meso-, macro- and micromeres, were measured at the 16-cell stage. The averaged diameters and standard deviations of meso-, macro- and micromeres were 28.4±1.3 (n=15), 33.8±3.9 (n=10) and 21.2±3.6 μm (n=10), respectively. Next, embryos were dissociated into single blastomeres every hour from 5 to 8 hr postfertilization, and the diameter of dissociated blastomeres were measured (Fig. 3). From the diameters of ancestor blastomeres, the diameter of blastomeres during later cleavage stages can be calculated. For example, the diameter of blastomeres in macromere lineage after the 6th cleavage is obtained by dividing 33.8 with 1.26^2. On the histograms of blastomere diameters, the calculated diameters in each lineage are indicated with arrows accompanying the number of each cleavage cycle.

At 5 hr postfertilization, most of blastomeres completed the 6th cleavage, while some did not divide yet (Fig. 3A). Small micromeres were first observed at this time (indicated by ‘s-mic’ in Fig. 3A). At 6 hr postfertilization, a portion of blastomeres had already undertaken the 7th cleavage (Fig. 3B). By the 7th hr of development, embryos had completed the 7th cleavage (Fig. 3C). At the 8th hr of development, most of blastomeres seem to have undertaken the 8th

cleavage (Fig. 3D). Taking these data into consideration, presumed periods of the 6th, 7th and 8th cleavages were estimated as shown in Fig. 2 (both-sided arrows). From diameters of the dissociated blastomeres, it was also elucidated that embryos had not completed the 10th cleavage even at the late gastrula stage (24 hr, Fig. 3E).

Initiation of asynchronous cleavage

In *H. pulcherrimus* embryos, division of blastomeres becomes asynchronous from the 8th cleavage onward (Masuda and Sato, 1984). In contrast to this, the data shown in Fig. 2 and 3 suggest that the division becomes asynchronous from the 6th or 7th cleavage onward in *E. mathaei* embryos. However, the possibility remains that the broad distribution of blastomere diameters merely reflects the asynchrony among embryos.

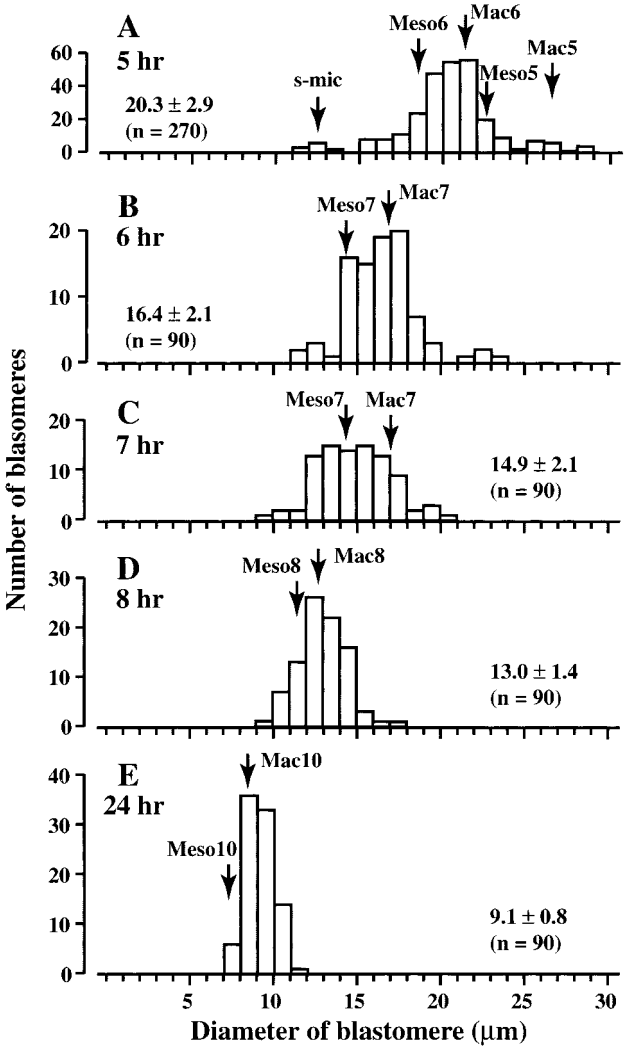

Fig. 3. *Distribution of the size of blastomeres during later cleavages*
X-axis: diameter of blastomere (μm). Y-axis: number of blastomeres. A: data obtained at 5 hr postfertilization. B: 6 hr. C: 7 hr. D: 8 hr. E: 24 hr. The calculated diameters of blastomeres after the completion of each cleavage are indicated with arrows with individual notations. Mac5–10: macromere lineage. Meso5-10: mesomere lineage. s-mic: small micromeres formed around the 6th cleavage.

To ascertain the timing of the initiation of asynchronous cleavage, individual embryos were observed by staining the nuclei with DAPI (Fig. 4). The 4th cleavage was almost synchronous. In some embryos, divisions of the animal blastomeres occurred slightly earlier than those of the vegetal blastomeres (Fig. 4A-A"); the difference was 5 min at most. Synchrony in the 5th cleavage seemed to be lost to some extent (Fig. 4B-B"), but the difference in the occurrence of cleavages was still within 5–10 min. In the embryo shown in Fig. 4C-C", most of the nuclei in the animal hemisphere are in prophase or metaphase of the 6th cleavage, while the nuclei in the vegetal hemisphere still remain in prophase. Thus, synchrony of cleavages in each hemisphere seemed to be retained up to the 6th cleavage, although difference in the timing of cleavages was noticed between the animal and vegetal hemispheres. However, the occurrence of the 7th cleavages was asynchronous among the blastomeres even in the same lineage, as shown in Fig. 4D-D". Nuclei of some blastomeres are in metaphase or anaphase, while the others are in S-phase even in the same hemisphere. Together with the distribution of blastomere diameters shown in Fig. 3, these data indicate that cleavages become asynchronous from the 7th cleavage onward in *E. mathaei* embryos, one cycle earlier than in *H. pulcherrimus*.

Increase in cell number after hatching

E. mathaei embryos hatched out from the fertilization membrane around the 9th hr of development. After hatching, nuclei of embryonic cells could be clearly stained with aceto-orcein, probably due to the tight packaging of chromosomes (Rowland and Rill, 1987). Fig. 5 shows change in the number of cells per embryo from 9 to 48 hr. From this figure, it is clear that the 9th cleavage had already started at 9 hr postfertilization. However, the completion of the 9th cleavage was around 15 hr. The 10th cleavage still continued even in the late gastrulae (24 hr). This coincides well with the results obtained from the measurement of the diameters of dissociated blastomeres (Fig. 3E). In the pluteus-stage embryo (48 hr), about two thirds of constituent cells had undertaken the 11th cleavage.

In *H. pulcherrimus*, embryos hatch out after the 10th cleavage and develop into the late gastrula around the completion of the 11th cleavage (Kominami, 2000). Therefore, the timings of hatching out and the completion of gastrulation in *E. mathaei* embryos are also earlier by one cell cycle than those in *H. pulcherrimus*.

Number of primary mesenchyme cells

As described above, the asynchronous cleavage, hatching out and gastrulation in *E. mathaei* started one cell cycle earlier than those in well-known sea urchins. As a result, the late-gastrula stage embryo of *E. mathaei* was composed of only several hundreds of cells. These seem to be ascribed to the small size of *E. mathaei* eggs. As is well

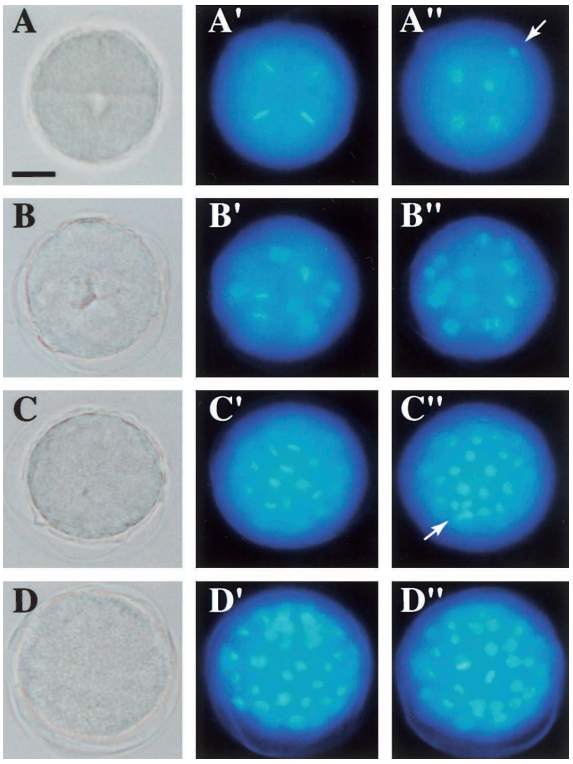

Fig. 4. *Synchrony of cleavages examined with DAPI staining*
A-A": 4th cleavage. B-B": 5th cleavage. C-C": 6th cleavage. D-D": 7th cleavage. A-D: bright field images. A'-D': fluorescence images focused at the animal hemisphere. A"-D": fluorescence images focused at the vegetal hemisphere. An arrow in A" indicates the sperm head attached to the fertilization envelope. An arrow in C" indicates the cluster of cells in small micromere lineage. Scale bar in A indicates 20 μm.

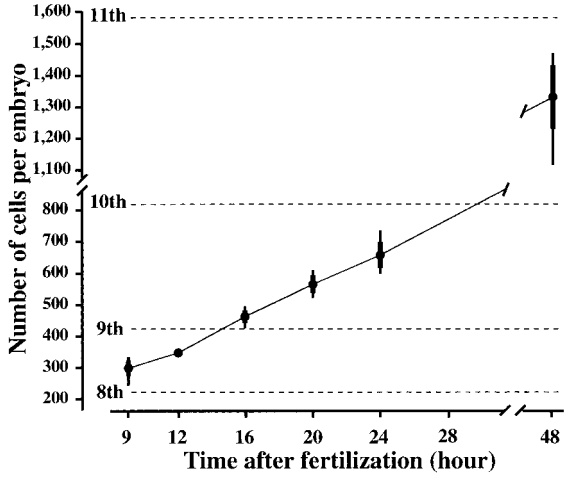

Fig. 5. *Change in the number of cells in whole embryos*
X-axis: time after fertilization (hr). Y-axis: number of cells per embryo. Solid circle: averaged number of constituent cells. Thin and thick vertical bars indicate the distribution range and standard deviation, respectively. At each observation point, 12 embryos were examined. Horizontal dotted lines indicate the numbers of cells after the completion of individual cleavages. The numbers were calculated based on the following assumptions. (1) All the descendants of meso- or macromeres divide at each cleavage cycle. (2) Blastomeres in large micromere lineage divide three times at the 7th, 8th and 9th cleavage stage. (3) Small micromeres divide once around the 9th cleavage.

known, division schedule of blastomeres in micromere lineage is independent of meso- and macromere lineages. Therefore, it is interesting to know whether the size of eggs affect the division and differentiation schedule of blastomeres in micromere lineage.

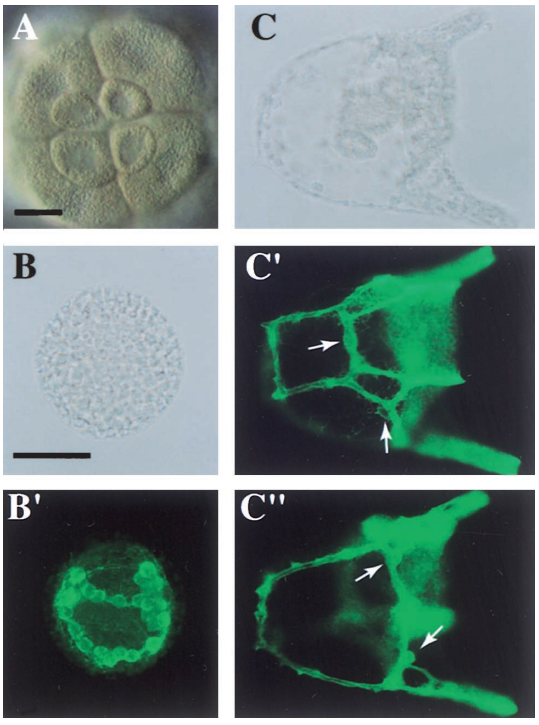

Fig. 6. *Micromeres and primary mesenchyme cells*
A: differential interference contrast image of a 16-cell stage embryo (vegetal view). B, B': at the early gastrula stage (20 hr postfertilization). C-C": at the pluteus stage (44 hr). B, C: bright field images. B', C' and C": fluorescence images. Arrows in C' and C" indicate PMCs. Scale bar in A indicate 20 μm. Scale bar in B is common to B' and C-C", and indicates 50 μm.

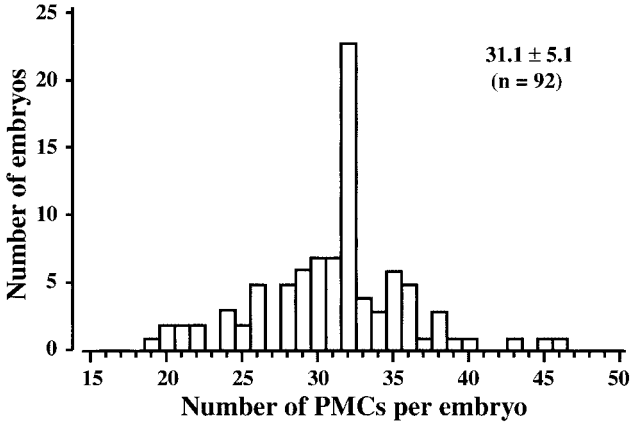

Fig. 7. *Number of primary mesenchyme cells at the early gastrula stage*
X-axis; number of primary mesenchyme cells (PMCs) per embryo. Y-axis; number of embryos. Numerals at the right top corner are the averaged number of PMCs ± standard deviation (number of embryos examined). The embryos containing 32 PMCs were most frequently observed.

Relative size of micromeres formed at the 16-cell stage seemed to be somewhat larger than those in other sea urchins (Fig. 1C). Further, the size of four micromeres in an embryo was fairly variable in a considerable portion of embryos (Fig. 6A). As shown in Fig. 6B, B' (at the early gastrula stage), PMCs are rather large in diameter, compared with other embryonic cells. At the pluteus stage, a well-developed larval skeleton was formed (Fig. 6C-C"). Although the contour of PMCs was scarcely noticed, a small number of PMCs could be demarcated even at the pluteus stage (arrows in C' and C"). The diameters of such PMCs did not differ from those observed at the early gastrula stage.

As shown in Fig. 7, the number of PMCs obtained at the early gastrula stage was fairly variable among embryos. The maximum number was 46. The embryo containing only 19 PMCs was also observed. The average was 31.1 with a standard deviation of 5.1. It is of note that the embryos having 32 PMCs were frequently observed.

Pseudopodia formation during early cleavage stage

The results described above raised the possibility that much earlier events would also occur earlier by one cell cycle. As reported, sea urchin blastomeres form lobopodium-like pseudopodia when embryos are dissociated into single blastomeres in the presence of Ca^{2+} (Masui and Kominami, 2001). In *H. pulcherrimus*, the timings of such pseudopodia formation in meso-, macro- and micromere lineage are 5th, 6th and 4th cleavage, respectively.

Up to the 8-cell stage, dissociated blastomeres of *E.*

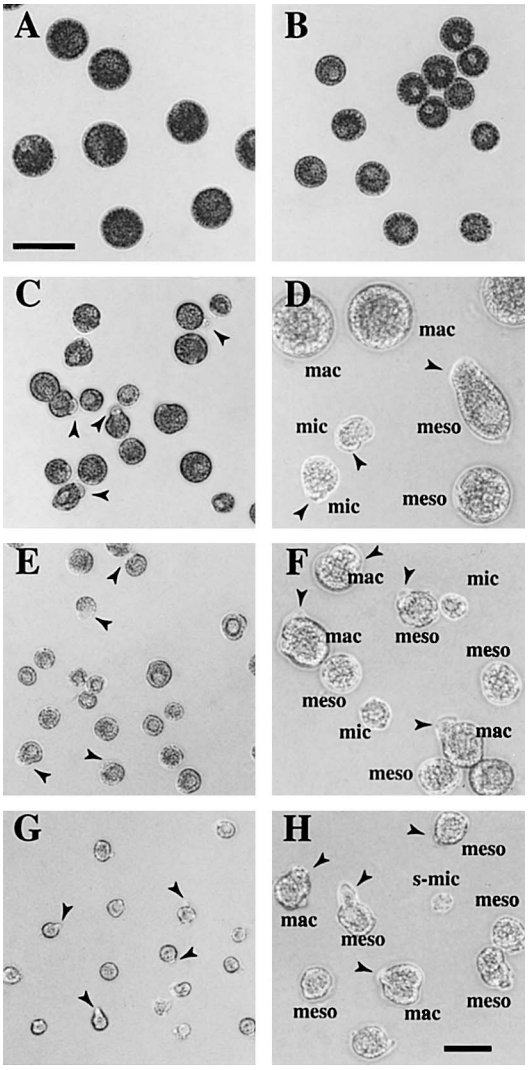

Fig. 8. *Pseudopodia formation in dissociated blastomeres*
A: 4-cell stage. B: 8-cell stage. C, D: 16-cell stage. E, F: 32-cell stage. G, H: 60-cell stage (after the 6th cleavage). Arrowheads indicate pseudopodia. Notations, mac, meso and mic indicate the blastomeres in macro-, meso- and micromere lineages, respectively. Scale bar in A is common to B, C, E and G, and indicates 20 μm. Scale bar in H is common to D and F, and indicates 10 μm.

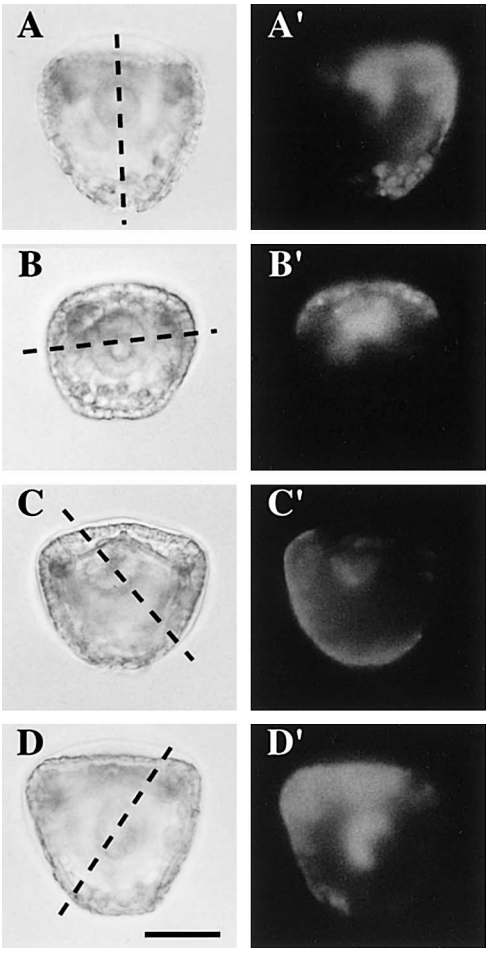

Fig. 9. *Lucifer Yellow-injected embryos observed at the late gastrula or early prism stage*
A, A': right half is labeled. B, B': ventral half is labeled. C, C': most of the dorsal part and small ventral part is labeled (Dorso-lateral (L) labeling pattern). D, D': most of the ventral part and small dorsal part is labeled (Ventro-lateral (L) labeling pattern). A-D: bright field images. A'-D': fluorescence images (blue light excitation). Dotted lines in A-D indicate the boundaries between labeled and non-labeled regions, i.e., the plane of the first cleavage. Scale bar indicates 50 μm.

Table 1. Number of embryos showing respective labeling patterns

Labeling pattern	Coinciding or Perpendicular				Oblique			
	Left half	Right half	Ventral half	Dorsal half	Dorso-lateral (L)	Ventro-lateral (R)	Ventro-lateral (L)	Dorso-lateral (R)
Series I	2	2	5	5	3	0	0	1
Series II	2	1	4	1	0	0	1	2
Series III[a)]	2	1	9	4	1	1	1	3
Subtotal	6	4	18	10	4	1	2	6
Complementary patterns	10[b)]		28[b)]		5		8	
Rectangular of oblique	38[c)]				13[c)]			

[a)] Data obtained from 5 batches of embryos are collected.
[b)] Difference between the values is statistically significant (test for the proportion; Z=2.76, p<0.01).
[c)] Difference between the values is statistically significant (Z=3.54, p<0.005).

mathaei embryos remained spherical and did not form pseudopodia at all (Figs. 8A; 4-cell stage and B; 8-cell stage). After the occurrence of the 4th cleavage, a considerable portion of mesomeres formed pseudopodia as well as micromeres (Fig. 8C, D). The pseudopodia are not mere the cytoplasmic blebs but show adhesive properties (Fig. 8D, arrowheads). The mesomere shown in Fig. 8D is elongated due to the adhesion to the substratum. After the occurrence of the 5th cleavage, most of blastomeres, including those in macromere lineage, formed pseudopodia (Fig. 8E, F). Almost all the blastomeres of 60-cell stage embryos showed extensive pseudopodia formation and became irregular in shape after dissociation (Fig. 8G, H). This observation shows that blastomeres of *E. mathaei* embryos in meso- and macromere lineages form pseudopodia after the occurrence of 4th and 5th cleavage, respectively. These timings in *E. mathaei* are earlier by one cell cycle than those in *H. pulcherrimus*.

Specification of dorso-ventral axis

When one of blastomeres of the 2-cell stage embryo was labeled in *H. pulcherrimus*, eight labeling patterns were observed at the prism stage with respect to the DV-axis (Kominami, 1988). This observation suggested that the DV-axis (oral-aboral axis) would be specified at some point from the 5th to 6th cleavage. It is of interest that this timing coincides well with the timings of the initiation of pseudopodia formation. As described above, some blastomeres of *E. mathaei* embryos begin to form pseudopodia, i.e., become adhesive from the 4th cleavage onward. Therefore, it is naturally supposed that the DV-axis is specified around the 16-cell stage and that only four labeling patterns (dorsal, ventral, left and right) would appear, if one of blastomeres is labeled at the 2-cell stage.

Fig. 9 shows examples of the labeled embryos observed at the late gastrula or early prism stage. In the embryo shown in Fig. 9A, A', the right half of the embryo was labeled with the fluorescent dye; the first cleavage plane coincides with the median plane of the embryo. In contrast to this, the first cleavage plane is perpendicular to the median plane in the embryo shown in Fig. 9B, B'. Likewise in *H. pulcherrimus*, 'oblique' labeling patterns were also observed. The embryo shown in Fig. 9C, C', most of the dorsal part and small ventral part (left side) were labeled (named as dorso-lateral (L) labeling). On the other hand, most of the ventral part and small dorsal part (left side) were labeled in the embryo shown in Fig. 9D, D' (ventro-lateral (L) labeling). In these two embryos, one of the 5th cleavage planes of the mesomeres had been employed as the median plane of embryos.

Table 1 summarizes the number of embryos classified with respective labeling patterns. Of interest, the embryos with 'coinciding' or 'perpendicular' pattern were more frequently observed than the embryos with oblique labeling patterns in every series of experiments (I–III). The difference in the numbers (38:13) was statistically significant (Z=3.54, p<0.005). This indicates that the 1st or 2nd cleavage plane is predominantly employed as the median plane of embryos, and suggests that the DV-axis is specified at the 16-cell stage in a majority of embryos. Another significant difference is found in the frequencies of appearance between coinciding and perpendicular labeling patterns. The difference in those numbers (10:28) is also statistically significant (Z=2.76, p<0.01), indicating that the 2nd cleavage plane is preferentially employed as the median plane of embryos rather than the 1st cleavage plane. Difference in the numbers of complementary labeling patterns, e.g., left: right (6:4), or ventral: dorsal (18:10), was not statistically significant.

DISCUSSION

Initiation of asynchronous cleavage

In these years, several reports have referred to the significance of the late blastula stage in sea urchin development. 'Early mRNAs', including those encoding tolloid and BMP-1, are transcribed during the late blastula stage (Reynolds *et al*., 1992). Presumptive endodermal cells require

cell contacts for their differentiation, but become to be able to fulfill their fate without further cell contact (Chen and Wessel, 1996). Specification of mesodermal tissues, such as pigment cells or blastocoelar cells, occurs also during late cleavage stages (Kominami, 1998, 2000; McClay *et al*., 2000; Sweet *et al*., 2002). Thus, the basic body plan of future embryos seems to be established during late cleavage stages. However, many problems remain unsolved concerning the events occurring during late cleavage stages. Presently, much more information is necessary for the comprehensive understanding of sea urchin development.

One of the unsolved problems is the nature of MBT in sea urchin embryos. Unlike in *Xenopus* embryos, it has not been characterized what factors affect the transition from synchronous to asynchronous cleavage, probably due to the difficulty in manipulating unfertilized or fertilized eggs. In the present study, we used the difference in the egg volume among sea urchin species to overcome the difficulty. As revealed in the present study, cleavages become asynchronous from the 7th cleavage in *E. mathaei* embryos (Figs. 2, 3 and 4), one cell cycle earlier than in *H. pulcherrimus* (Masuda and Sato, 1984), while the egg volume of the former species is about one half to that of the latter. This suggests that the nucleo-cytoplasmic ratio is important in directing the timing of the transition as in *Xenopus* embryos.

Timing of hatching and gastrulation

It is generally accepted that sea urchin embryos hatch out from the fertilization envelope after the completion of the 10th cleavage (Endo, 1966). Surprisingly, *E. mathaei* embryos had not complete the 9th cleavage by the hatching stage, hence the embryos contained only 290 cells (Fig. 5). Even at the late gastrula stage, all the constituent cells have not undertaken 10 cycles of cell divisions (Fig. 5). These suggest that neither the number of cleavage cycles nor DNA replications directs the timing of hatching or progress of gastrulation.

From the present study, it cannot be distinguished which factor, a cytoplasmic oscillator or the nucleo-cytoplasmic ratio, is crucial in directing the timing of such events. As reported earlier (Matsumoto *et al*., 1988), the timings of hatching out and onset of gastrulation are directed with different timers; the timing of hatching is directed with the timer that begins to operate soon after fertilization and governs the cleavage cycles, while the timing of the onset of gastrulation seems to be directed with a timer that begins to operate after cleavages become asynchronous. Time schedule of early cleavages, i.e., occurrence of the first cleavage and cleavage intervals, does not differ between *E. mathaei* and *H. pulcherrimus*. Embryos of *H. pulcherrimus* hatch out around 12 hr and begin to gastrulate at about 16–17 hr postfertilization. On the other hand, *E. mathaei* embryos hatch out around 9 hr and begin to gastrulate at about 18 hr postfertilization (Fig. 1G). Thus, the relative time length from hatching to the initiation of gastrulation is quite different between these two species. This supports the idea that the timings of hatching and onset of gastrulation are directed with different timing mechanisms.

Number of cell divisions in micromere lineage

Some data are available on the numbers of PMCs in different sea urchin species. In *Clypeaster japonicus*, the number ranged from 55 to 75 (Takahashi and Okazaki, 1979). In *Lytechinus variegatus*, the number of PMCs was reported to be 60–64 (Ettensohn and McClay, 1988). In *H. pulcherrimus*, the averaged number were 50–60, although the number varied to some extent among batches of embryos (Kominami and Takaichi, 1998). Thus, the number of PMCs in well-known sea urchin species is around 60. These indicate that each micromere generally divides four times and give rise to nearly 16 PMCs before they form the larval skeleton. In contrast to this, each micromere divides only three times and produces 8 PMCs in *E. mathaei* embryos, since the total number of PMCs is around 32 (Fig. 7).

The size of differentiated PMCs was almost the same as far as examined on the antibody-stained specimens (Fig. 6B'). It is important to remember that *E. mathaei* embryos sometimes form extreme large micromeres as shown in Fig. 6A. Such micromeres might be able to undergo four rounds of cell divisions. If embryos form one or two larger micromeres, the number of PMCs will be around 40 or 48, respectively. In fact, such numbers of PMCs were observed in some embryos (Fig. 7). On the contrary, if two smaller micromeres are formed, the number will be around 24. The embryos containing such number of PMCs were also observed (Fig. 7). Therefore, differentiation of PMC does not strictly depend on the number of division cycles or DNA replications. In another words, the number of cell divisions depends on the volume of micromeres (Yamada and Nishida, 1999).

In addition to say, the monoclonal antibody used in this study was raised against *H. pulcherrimus* embryos (Kominami and Takaichi, 1998). Nonetheless, the antibody binds specifically to the surface of PMCs in *E. mathaei*. The antibody used in this study recognizes the molecules similar to msp130 (Leaf *et al*., 1987; Anstrom *et al*., 1987). Such molecules seem to prevail in a variety of sea urchins.

Timing of the initiation of close cell contact

As shown in the present study, blastomeres in meso- and macromere lineages began to form lobopodium-like pseudopodia after the 4th and 5th cleavage, respectively (Fig. 8). These timings are earlier by one cell cycle than in *H. pulcherrimus*. Since the egg volume of *E. mathaei* is about one half to that of *H. pulcherrimus*, it is naturally supposed that the timing of pseudopodia formation is directed with a nucleo-cytoplasmic ratio. More strictly speaking, the nucleus-cell volume ratio (not the nucleo-cytoplasmic ratio) would be crucial in directing the timing (Masui and Kominami, 2001). When blastomeres become adhesive, the ratio exceeded 0.1 irrespective of the blastomere lineage in *H.*

pulcherrimus. This is also the case in starfish embryos, while the definite value was 0.06 (Masui *et al*., 2001). Unfortunately, we could not obtain enough data on the change in the nucleus-cell volume ratio, since it was difficult to identify the lineage of dissociated blastomeres in *E. mathaei*. To clarify the properties of the developmental timer that directs the initiation of close cell contact, it is necessary to obtain the quantitative data on the change in the nucleus-cell volume ratio also in *E. mathaei*.

Specification of dorso-ventral axis

It is still a debated problem when the DV-axis of sea urchin embryos is specified (Henry, 1998), since the axis is labile (Coffman and Davidson, 2001). Further, the relationship between the first cleavage plane and the median plane of embryos, which is an indicator that shows the timing of the DV-axis specification, varies among sea urchin species (Kominami, 1988; Cameron *et al*., 1989; Henry *et al*., 1990, Summers *et al*., 1996). In the direct developing sea urchin *Heliocidaris erythrogramma*, the DV-axis is specified prior to the 1st cleavage, and thought to be specified even in the unfertilized egg (Henry *et al*., 1990). In indirect developing sea urchins, however, many reports support the idea that the DV-axis is specified through cell-cell interactions during early cleavage stage. This is also the case in the starfish *Asterina pectinifera* (Kominami, 1983). It is of note that vegetal hemisphere play an important role in the specification of DV-axis during early cleavage stages. In *Psammechinus miliaris*, the animal half isolated at the 8-cell stage differentiates into a permanent blastula that does not show any sign of DV-axis. On the other hand, the animal halves isolated at the 32-cell stage develop into the blastulae having a depression that resembles the stomodaeum formed in normal embryos (Hörstadius, 1973).

Like in *H. pulcherrimus* embryos, oblique labeling patterns were observed also in *E. mathaei* embryos (Fig. 9, Table 1). However, the 1st or 2nd cleavage plane was preferentially employed as the median plane (Table 1). This suggests that the DV-axis is specified at the 4th cleavage rather than the 5th cleavage, one cell cycle earlier than in *H. pulcherrimus*, of which egg volume is twice that of *E. mathaei*. Further, the inclination was observed that the 2nd cleavage plane was more frequently employed as the median plane of embryos (Table 1). Probably, the immediately preceding cleavage plane is easy to be employed as the median plane of the embryo. These may also suggest that specification of the DV-axis needs close contact of blastomeres. It should be emphasized that the timing of DV-axis specification coincides well with the timing when blastomeres become adhesive (Fig. 8). In another words, the timings of the DV-axis specification and the initiation of close cell contact might be directed by the same factor, i.e., the nucleo-cytoplasmic ratio.

Thus, the obtained results suggest that the timings of early developmental events in sea urchin embryos are mostly under the control of nucleo-cytoplasmic ratio (or nucleus-cell volume ratio). In the present study, timing mechanisms was studied by means of comparison among sea urchin species, instead of manipulations. Although attention should be paid in interpreting the results obtained from such comparison, the method would help us to reveal new aspects of the unsolved problems that cannot be addressed with the ordinary methods.

ACKNOWLEDGMENT

We would express sincere thanks to Professor. Y. Yanagisawa, Ehime University, for providing us the facility in collecting animals. We also thank all the members of our laboratory for their collaboration.

REFERENCES

Anstrom JA, Chin JE, Leaf DS, Parks AL, Raff RA (1987) Localization and expression of msp130, a primary mesenchyme lineage-specific cell surface protein in the sea urchin embryo. Development 101: 255–265

Cameron RA, Fraser SE, Britten RJ, Davidson EH (1989) The oral-aboral axis of a sea urchin embryo is specified by first cleavage. Development 106: 641–647

Chen SW, Wessel GM (1996) Endoderm differentiation in vitro identifies a transitional period for endoderm ontogeny in the sea urchin embryo. Dev Biol 175: 57–65

Coffman JA, Davidson EH (2001) Oral-aboral axis specification in the sea urchin embryo. I. Axis entrainment by respiratory asymmetry. Dev Biol 230: 18–28

Dan K, Ikeda M (1971) On the system controlling the time of micromere formation in sea urchin embryos. Dev Growth Differ 13: 285–301

Endo Y (1966) Fertilization, cleavage and early development. In "Contemporary Biology: Development and Differentiation vol 4" Ed by Isemura *et al*., Iwanami Shoten, Tokyo, pp 1–61

Ettensohn CA, McClay DR (1988) Cell lineage conversion in the sea urchin embryo. Dev Biol 125: 396–409

Henry JJ, Wray GA, Raff RA (1990) The dorsoventral axis is specified prior to first cleavage in the direct developing sea urchin *Heliocidaris erythrogramma*. Development 110: 875–884

Henry JJ (1998) The development of dorsoventral and bilateral axial properties in sea urchin embryos. Semin Cell Dev Biol 9: 43–52

Hörstadius S (1973) "Experimental embryology of echinoderms", Oxford University Press (Clarendon), London

Kominami T (1983) Establishment of embryonic axes in larvae of the starfish, *Asterina pectinifera*. J Embryol Exp Morph 75: 87–100

Kominami T (1988) Determination of dorso-ventral axis in early embryos of the sea urchin, *Hemicentrotus pulcherrimus*. Dev Biol 127: 187–196

Kominami T (1998) Role of cell adhesion in the specification of pigment cell lineage in embryos of the sea urchin, *Hemicentrotus pulcherrimus*. Dev Growth Differ 40: 609–618

Kominami T, Takaichi M (1998) Unequal divisions at the third cleavage increase the number of primary mesenchyme cells in sea urchin embryos. Dev Growth Differ 40: 545–553

Kominami T (2000) Establishment of pigment cell lineage in embryos of the sea urchin, *Hemicentrotus pulcherrimus*. Dev Growth Differ 42: 41–51

Leaf DS, Anstrom JA, Chin JE, Harkey MA, Showman RM, Raff RA (1987) Antibodies to a fusion protein identify a cDNA clone encoding msp130, a primary mesenchyme-specific cell surface protein of the sea urchin embryo. Dev Biol 121: 29–40

Masuda M, Sato H (1984) Asynchronization of cell divisions concurrently related with ciliogenesis in sea urchin blastulae. Dev Growth Differ 26: 281–294

Masui M, Kominami T (2001) Change in the adhesive properties of blastomeres during early cleavage stages in sea urchin embryo. Dev Growth Differ 43: 43–53

Masui M, Yoneda M, Kominami T (2001) Nucleus: cell volume ratio directs the timing of the increase in blastomere adhesiveness in starfish embryos. Dev Growth Differ 43: 295–304

Matsumoto Y, Kominami T, Ishikawa M (1988) Timers in early development of sea urchin embryos. Dev Growth Differ 30: 543–552

McClay DR, Peterson RE, Range RC, Winter-Vann AM, Ferkowicz MJ (2000) A micromere induction signal is activated by beta-catenin and acts through notch to initiate specification of secondary mesenchyme cells in the sea urchin embryo. Development 127: 5113–5122

Newport J, Kirschner M (1982a) A major developmental transition in early *Xenopus* embryos. I. Characterization and timing of cellular changes at the midblastula stage. Cell 30: 675–686

Newport J, Kirschner M (1982b) A major developmental transition in early *Xenopus* embryos. II. Control of the onset of transcription. Cell 30: 687–696

Reynolds SD, Angerer LM, Palis J, Nasir A, Angerer RC (1992) Early mRNAs, spatially restricted along the animal-vegetal axis of sea urchin embryos, include one encoding a protein related to tolloid and BMP-1. Development 114: 769–786

Rowland RD, Rill RL (1987) Atypical changes in chromatin structure during development in the sea urchin, *Lytechinus variegatus*. Biochim Biophys Acta 908: 169–178

Satoh N, Ikegami S (1981a) A definite number of aphidicolin-sensitive cell-cyclic events are required for acetylcholinesterase development in the presumptive muscle cells of the ascidian embryos. J Embryol Exp Morph 61: 1–13

Satoh N, Ikegami S (1981b) On the 'clock' mechanism determining the time of tissue-specific enzyme development during ascidian embryogenesis. J Embryol Exp Morph 64: 61–71

Satoh N (1985) Recent advances in our understanding of the temporal control of early embryonic development in amphibians. J Embryol Exp Morph 89: Suppl 257–270

Showman RM, Foerder CA (1979) Removal of the fertilization membrane of sea urchin embryos employing aminotriazole. Exp Cell Res 120: 253–255

Soll DR (1979) Timers in developing systems. Science 203: 841–849

Soll DR (1983) A new method for examining the complexity and relationships of 'timers' in developing systems. Dev Biol 95: 73–91

Summers RG, Piston DW, Harris KM, Morrill JB (1996) The orientation of first cleavage in the sea urchin embryo, *Lytechinus variegatus*, does not specify the axes of bilateral symmetry. Dev Biol 175: 177–183

Sweet HC, Gehring M, Ettensohn CA (2002) LvDelta is a mesoderm-inducing signal in the sea urchin embryo and can endow blastomeres with organizer-like properties. Development 129: 1945–1955

Takahashi MM, Okazaki K (1979) Total cell number and number of primary mesenchyme cells in whole, 1/2 and 1/4 larvae of *Clypeaster japonicus*. Dev Growth Differ 21: 553–566

Yamada A, Nishida H (1999) Distinct parameters are involved in controlling the number of rounds of cell division in each tissue during ascidian embryogenesis. J Exp Zool 284: 379–391

(Received January 27, 2003 / Accepted March 10, 2003)